

Conformations and Hydrogen-Bonded Complexes of Aminoethanol: A Matrix Isolation and *Ab Initio* Study

Shivangi Vaish
MS14070

*A dissertation submitted for the partial fulfillment of BS-MS dual
degree in science*



**Indian Institute of Science Education and Research Mohali
April 2019**

Certificate of Examination

This is to certify that the dissertation titled “**Conformations and Hydrogen-Bonded Complexes of Aminoethanol: A Matrix Isolation Infrared and *Ab Initio* Study**” submitted by **Ms. Shivangi Vaish** (Reg. No. MS14070) for the partial fulfillment of BS-MS dual degree programme of the institute, has been examined by the thesis committee duly appointed by the institute. The committee finds the work done by the candidate satisfactory and recommends that the report be accepted.

Dr.Sugumar Venkataramani

Dr. P. Balanarayan

Prof. K. S. Viswanathan
(Supervisor)

Dated: April 26, 2019

Declaration

The work presented in this dissertation has been carried out by me with Prof. K.S. Viswanathan at the Indian Institute of Science Education and Research Mohali.

This work has not been submitted in part or in full for a degree, a diploma, or a fellowship to any other university or institute. Whenever contributions of others are involved, every effort is made to indicate this clearly, with due acknowledgement of collaborative research and discussions. This thesis is a bonafide record of original work done by me and all sources listed within have been detailed in the bibliography.

Shivangi Vaish
(Candidate)

Dated: April 26, 2019

In my capacity as the supervisor of the candidate's project work, I certify that the above statements by the candidate are true to the best of my knowledge.

Prof. K. S. Viswanathan
(Supervisor)

Acknowledgement

I would like to thank all those who helped me in some way, directly or indirectly to complete this work. First and foremost, I would like to thank Prof. K. S. Viswanathan, my thesis guide for making me a part of his group, engaging me in new ideas, supporting me at times and guiding me over this past year. Thanks, is a too mild word to express my feelings of indebtedness.

I also thank Dr. Sugumar Venkataramani and Dr. P. Balanarayan for being a part of my thesis committee and for their valuable inputs and suggestions for my work.

I must thank IISER Mohali for all the facilities and opportunities and DST for the INSPIRE fellowship.

This work would not have been possible as easily without the help and guidance in understanding the computational and experimental setup from my seniors in the lab; Jyoti and Pankaj. A big thanks to my lab members; Himanshi, Jai and Dipali for providing a great lab environment to work in. Also, thanks to the POC lab members for their scientific and nonscientific help over the last year.

I would like to acknowledge my friends; Ritika and Akanksha who were there to support me all the time; Parth for always having my back; Vaishnavi for all the fun times; Jaideep, Misbah and Nishant for being such nice friends all this while; Prachi for maintaining just the right amount of insanity I needed. Thank you, Aman, for the endless encouragement and understanding throughout the whole journey of last few years.

I would also like to acknowledge my parents Rajan Kumar and Aarti and also my brother Sathak for being there for me all the time and providing me with unfailing love and support throughout my years of study. This all would not have been possible with them. Thank You

List of Figure

Figure No.	Figure Caption	Page No.
2.1	Cartoon Description of Matrix Isolation	5
2.2	Schematic diagram for cryo-system assembly	7
2.3	Cryostat and its associated units	7
2.4	Diffusion Pump	8
2.5	FTIR Spectrometer	9
2.6	Home built Matrix Isolation setup	9
3.1	Geometry optimization to find minima	13
4.1	Chemical Structure of aminoethanol	15
4.2	Nomenclature scheme for aminoethanol conformers	16
4.3	Conformations of aminoethanol	16
4.4	AIM analysis of aminoethanol	17
4.5	Matrix isolation IR spectrum of aminoethanol (black) in nitrogen matrix along with the computed scaled spectra (red) for gg'g showing the (a) O-H stretching frequency region; (b) C-O & C-N stretching frequency region.	21
4.6	Matrix isolation IR spectrum (black) of aminoethanol in Argon matrix along with the computed scaled spectra (red) for gg'g showing the (a) O-H stretching frequency region; (b) C-O & C-N stretching frequency region.	23
4.7	Complexes of aminoethanol with water(above). AIM analysis for aminoethanol- water complexes (bottom)	24

List of Tables

Table No.	Table Caption	Page No.
3.1	Levels of theories	11
3.2	Basis Sets	12
4.1	Relative energy ordering for the conformers (kcal/mol)	17
4.2	NBO analysis for aminoethanol	19
4.3	Vibrational feature assignment Aminoethanol in Nitrogen matrix as per scaled computed frequencies obtained at MP2/aug-cc-pVDZ level of theory	21
4.4	Vibrational feature assignment aminoethanol in the argon matrix as per scaled computed frequencies obtained at MP2/aug-cc-pVDZ level of theory	22
4.5	Interaction energy (zero point corrected in kcal/mol) for aminoethanol water complex computed at MP2/aug-cc-pVDZ level of theory.	25
4.6	AIM analysis, showing the electron density and Laplacian values, for the aminoethanol water complexes	26
4.7	NBO analysis for aminoethanol-water complex	27
A.1	Dihedral angles for aminoethanol conformations	33
A.2	Bond length in aminoethanol conformers	33
A.3	Bond angles for aminoethanol conformations	34

List of Abbreviations

FTIR	Fourier Transfer Infrared
SP	Stationary Point
Elec	Electrostatic
Dis	Dispersive
Pol	Polarization
Ind	Inductive
Rep	Repulsive
UV	Ultra Violet
GM	Gifford-McMahon
KBr	Potassium Bromide
HF	Hartree-Fock
MP	Møller–Plesset perturbation theory
DFT	Density Functional Theorem
CC	Coupled cluster
FWHM	Full width at half maximum
ZPE	Zero point energy
ZPCE	Zero point corrected energy
AIM	Atoms-in-molecules
CP	Critical point
NBO	Natural Bond Orbital
STO	Slater Type Orbital

Contents

List of Figures	i
List of Tables	ii
Abbreviations	iii
Abstract	vi
Introduction	1
Experimental Method	3
The Technique of Matrix Isolation	3
Nature of Matrix	3
Matrix Isolated Species and its analysis	3
Matrix Isolation FTIR spectroscopy	4
Matrix Isolation infrared setup	6
Cryostat	6
Vacuum System	6
Sample Introduction Assembly	8
FTIR Spectrometer	8
Computational Method	10
Introduction	10
Levels of theory	10
Basis Set	11
Geometry Optimization and Frequency Calculation	12
Natural Bonding Orbital Analysis	13
AIM analysis	14
Results and Discussion	15
Aminoethanol Conformations	15
Computational Results	15
Experimental Results	20

Aminoethanol – Water Complex	24
Conclusions	28
References	30
Appendix	33

Abstract

Aminoethanol, a molecule with both amino and hydroxyl group on vicinal carbon atoms, has been studied in the literature. Due to the presence of the amino and hydroxyl groups, it has been an interesting molecule to study for the hydrogen bonding point of view as an interplay of inter and intramolecular hydrogen bonding can be observed in aminoethanol, an aspect that has not been well addressed in the previous work. The intermolecular hydrogen bonding of the aminoethanol - water system is also interesting to study as there are several isomers of this system.

Matrix Isolation infrared spectroscopy has been used to study the conformations of the aminoethanol in argon and nitrogen matrices. Lowest energy conformation has been observed in both the matrices. The conformations of aminoethanol have been studied computationally using different levels of theories, AIM and NBO analysis.

The aminoethanol water complexes have also been studied computationally, and the optimized structures for the water complexes corresponding to the lowest energy structure are presented. The orbital interaction analysis has also been performed to understand the role of orbital interactions in the structure of the complexes.

Chapter – 1

Introduction

“The hydrogen bond is an attractive interaction between a hydrogen atom from a molecule or a molecular fragment X-H in which X is more electronegative than H, and an atom of a group of atoms in the same or different molecule, in which there is an evidence of bond formation.” - definition of hydrogen bond proposed by the International Union of Pure and Applied Chemistry in 2011¹.

The studies of inter and intramolecular hydrogen bonded compounds in the Earth's atmosphere have received increased attention as vibrational transitions in these hydrogen bonded species have been shown to be important in the absorption of solar radiation and atmospheric photochemistry²⁻⁵. Hydroxy and amino groups rank among the most important hydrogen bond building blocks in nature. Aminoethanol molecule contains both amino and hydroxy group separated by two sp³-carbons. Due to such a structure, it is interesting to study the interplay of inter and intramolecular hydrogen bonding in aminoethanol. Aminoethanol is a triple rotor molecule due to which 27(3³) conformations are possible for it which makes it an interesting subject to study the conformations as well.

Aminoethanol is vital in an environmental perspective as it is considered as a benchmark solvent for the post-combustion carbon dioxide capture⁶. An aqueous solution of aminoethanol is also used in industries for carbon dioxide sequestration.

Infrared spectroscopy is a very useful method to investigate hydrogen bonds as one can observe the redshifts in the stretching frequencies of the bonds involved in hydrogen bond formation.

Intramolecular hydrogen bonding in aminoethanol has been the subject of many experimental and computational studies⁷⁻¹⁵. These studies include photoelectron spectroscopy, infrared spectroscopy, Raman spectroscopy, and microwave spectroscopy. These studies show weak hydrogen bonding interaction between the amino and the hydroxy group of aminoethanol making the gauche conformer more stable.

Matrix isolation infrared study done by Rasanen et al.⁹ on aminoethanol shows the intramolecular hydrogen bonded gauche conformer to be dominant which is supported by *ab initio* calculations done at STO-3G. They also studied photorotamerization occurring in the aminoethanol deposited in the matrix when it absorbs radiation of suitable frequencies.

Gas phase spectroscopic studies have also been done on aminoethanol, and they

show features corresponding to both free and hydrogen bonded O-H stretching^{10,15}. Gas phase vibrational spectroscopy experiments done by Thomsen et al. on aminoethanol showed the presence of intramolecular hydrogen bonding which was supported by the Non-Covalent Interaction(NCI) analysis done computationally¹⁵. Supersonic jet experiments were done on aminoethanol by Liu et. al¹⁴ also claim intramolecular hydrogen bonding in one of the conformers of aminoethanol.

The aminoethanol water complex is interesting to study from the hydrogen bonding point of view as multiple possibilities for proton donating and accepting sites exists. This system has been previously studied by Tubergen et al.¹⁶ using microwave spectroscopy and *ab initio* calculations. They observed the complexes with multiple intermolecular hydrogen bonding was more stable as compared to the ones with one inter and one intramolecular hydrogen bonding. Also, Haufa et al.¹⁷ did a study of the system using near IR spectroscopy to study the effect of water content on the molecular structure of aminoethanol molecule in the liquid phase and also did some DFT calculations corresponding to it. Not much work has been done on aminoethanol water system corresponding to the mid-IR region. This work, presented here, involves the *ab initio* calculations for geometry optimization and frequency calculation done on this system corresponding to the mid IR range.

This work covers the Matrix isolation FTIR and computational study of aminoethanol conformers. Along with that, the computational study of the aminoethanol water system has been presented in this work.

Chapter 2

Experimental Method

The Technique of Matrix Isolation

In the technique of matrix isolation, the sample molecules of interest are trapped in an inert gas-solid at a very low temperature and studied using a variety of spectroscopy tools. Nitrogen and noble gases such as Ar, Ne, Xe are used as matrix host materials, as they are chemically unreactive.

This technique was originally developed to trap and study the transient and reactive species such as free radicals. The idea of matrix isolation was first proposed by Pimental and co-workers¹⁸ during the mid-1950s. They intended to study free radicals, as these reactive species have a longer lifetime in the inert matrix, for want of a reaction partner. Matrix isolation requires high vacuum systems both to maintain the cryogenic temperatures and also to substantially eliminate impurities in the condensed matrix. Thus, the basis of the technique rests on two technologies: cryogenics and high vacuum systems.

Nature of matrix

To be used as a matrix, the substance must be chemically inert to the analyte molecule, rigid at the temperature of the experiment and transparent in the spectral region of interest. The temperature of the substrate, where the matrix is to be deposited is kept at a temperature below one-third of the melting point of the host gas to ensure the uniformity and the rigidity of the matrix. The matrix can be considered as a crystalline solid with grain boundaries, which are the regions for the defect. In the matrix, molecules of interest can be trapped and isolated in voids, defects or interstitial sites, due to which the site effect comes into play

Matrix Isolated Species and its analysis

The matrix gas is generally used in large excess with respect to the substrate molecules (1:1000). These dilute conditions are kept to ensure the isolation of the sample molecule with a negligible population of the dimers or the higher clusters. Once the solid matrix has been prepared, the trapped molecules are then studied using various experimental techniques such as FTIR, UV-Vis absorption, EPR, etc.

The solid matrix is assumed to present conditions where the trapped species are

immobile and devoid of any diffusion, as the temperature employed is way below the melting point of the matrix gas used. As there is no diffusion, the probability of reactions such as complex formation or dimerization is assumed to be negligible. Significant diffusion can, however, be observed when the temperature of the matrix is raised to about one-third of the melting point of the matrix host gas. This diffusion process can be used to advantage to study the intermolecular interactions as there will be an aggregation of the trapped species, provided these aggregates have significant intermolecular interactions that can be recognized through their characteristic spectral features. Generally, distinct spectral features show up due to these interactions which are very different from the spectral features of the monomers. Hence this can be used to study the weak interactions in the molecules. This process of warming up of the matrix is known as annealing. Annealing of the matrix can be done by raising the temperature of the matrix to one-third of the melting point of the matrix material so that it allows diffusion of molecules present in the matrix. The matrix can be then cooled back to the initial temperature, and the spectra can be recorded to identify if any new spectral features are emerging.

Matrix isolated FTIR spectroscopy

The technique of matrix isolation can be used to study the molecules and their interactions using the FTIR spectrophotometer. The infrared spectrum is the vibrational fingerprint of a molecule. In case of gas phase IR spectrum of a molecule, we can see the rotational lines along with the vibrational ones, with molecules populating a large number of rotational levels. This results in a large number of lines or a broad profile is often observed.

Also, the Doppler and collisional broadening come into play at higher temperatures. At the cryogenic temperatures, as in the matrix, both of these collisional factors are suppressed as molecules are frozen into the ground rovibronic state. The low temperature leads to the suppressing of rotation of the molecules, and also prevents diffusion of the trapped molecules, thus keeping them isolated. The major advantage of using this method is that it provides a reasonable uncongested spectrum with sharp line widths, with a full-width half minimum of nearly $2\text{-}5\text{ cm}^{-1}$, as opposed to linewidths which are at least an order or magnitude larger in solid and liquid samples. The sharp spectral peaks in the cryogenic matrix, help to study the weak interactions and conformers. The sample together with the inert gas is deposited on a solid substrate which is usually a window of material which is transparent in the spectral region; KBr, NaCl (transparency in region $400\text{ - }4000\text{ cm}^{-1}$), CsI

and CsBr (transparency in region $< 400 \text{ cm}^{-1}$) windows are usually used for studies in the infrared region.

As the sample molecules are isolated in inert matrices, the intermolecular interactions between the sample molecules are negligible, but their interactions with the matrix can not be ignored. Although the matrix is chemically inert, they do manifest subtle influences which are seen as shifts in the infrared frequencies compared with the gas phase data or as multiplets in the spectral structure. Shifts in the frequency ($\Delta\nu$) in the matrix as compared to the gas phase spectra are due to four primary factors: Electrostatic ($\Delta\nu_{\text{elec}}$), Inductive ($\Delta\nu_{\text{ind}}$), Dispersive ($\Delta\nu_{\text{dis}}$) and repulsive ($\Delta\nu_{\text{rep}}$).

$$\Delta\nu = \nu_{\text{matrix}} - \nu_{\text{gas}} = \Delta\nu_{\text{elec}} + \Delta\nu_{\text{ind}} + \Delta\nu_{\text{dis}} + \Delta\nu_{\text{rep}}$$

Where ν_{matrix} is the frequency of a given mode of a sample in the matrix and ν_{gas} is the frequency of that mode in the gas phase.

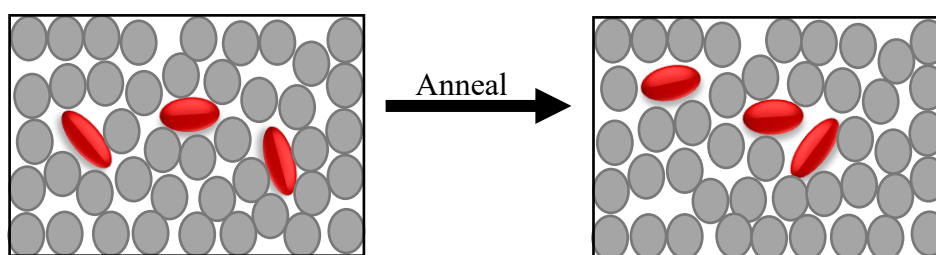


Figure 2.1: Cartoon description of matrix isolation

In an ideal matrix isolation experiment, it is desired to have isolation of the analyte molecules trapped in the matrix. Various factors like deposition rate and matrix ratio decide optimum isolation. At lower matrix to analyte ratio aggregates get trapped in the matrix and induce many spectral effects such as broadening, slight shifts and sometimes multiplets. The probability of isolation of a molecule occupying a single substitutional site can be calculated by using the formula, $P = (1-r)^{12}$. The probability of interaction is a chance of finding another molecule occupying one of the 12 sites that form the cage, P is the probability of another molecule not being present at those sites, and 'r' is reciprocal of the matrix ratio. For very high matrix ratios, i.e. very small value of 'r,' the above expression reduces to $P = 1 - 12r$, i.e., 99% isolation can be ensured with a matrix ratio of 1000.

Matrix Isolation infrared setup

The instrumentation of the matrix isolation set up involves the following components

1. Cryostat
2. Vacuum system
3. Sample Introduction Assembly
4. Fourier Transform Infrared (FTIR) Spectrometer

Cryostat

All our experiments were done at 12K for which we used a closed cycle helium compressor cooled cryostat from Sumitomo Heavy Industries Ltd. The cryostat used here works on the principle of Grifford McMahan (GM) cycle. The GM refrigeration cycle takes place at the cold head which is connected to the compressor through two gas lines for the flow of the working fluid, i.e., helium. High-pressure helium is supplied to the expander through one of the lines, and the other line returns the low-pressure helium. This flow of helium is maintained by the compressor. A vacuum shroud is constructed using stainless steel or Aluminum which makes it less vulnerable to adsorbing water. The vacuum shroud limits the heat load on the expander caused by conduction and convection. To measure and adjust the temperature of the sample deposited on the window a temperature controller (Lakeshore Instruments-Model 335) was used which was mounted near the cold window. In addition to this, a chiller unit is required to remove the heat from the low-pressure helium before returning it to the compressor. Fig 2.2 shows a general schematic for the closed cycle cryo-system assembly¹⁹. Fig. 2.3 shows the images of the cryostat and the associated units.

Vacuum System

High vacuum conditions (nearly 10^{-6} mbar) are required for the conduct of the matrix isolation experiments. In our experiment, we used a diffusion pump (Edwards, Diffstak MK2 series 100/300), backed up by a rotary pump (Hind Hivac, ED6) to attain the desired pressure (Fig. 2.4). The rotary pump is used to first obtain a pressure of nearly 10-3 mbar in the chamber, after which the diffusion pump is employed to further reduce the pressure to 10^{-6} mbar. Working of diffusion pump is based on momentum transfer to the gas molecules from a jet of oil. The heater vaporizes the oil which rises into the vapor chimney from where they are deflected downwards towards the pump walls which are then cooled by water from chiller flowing in a coil wound on the outer surface of the pump

chamber. The vacuum inside the system is measured using a digital Penning gauge (Hind Hivac) and a Pirani gauge 26(Edwards APG 100 Active Pirani gauge).

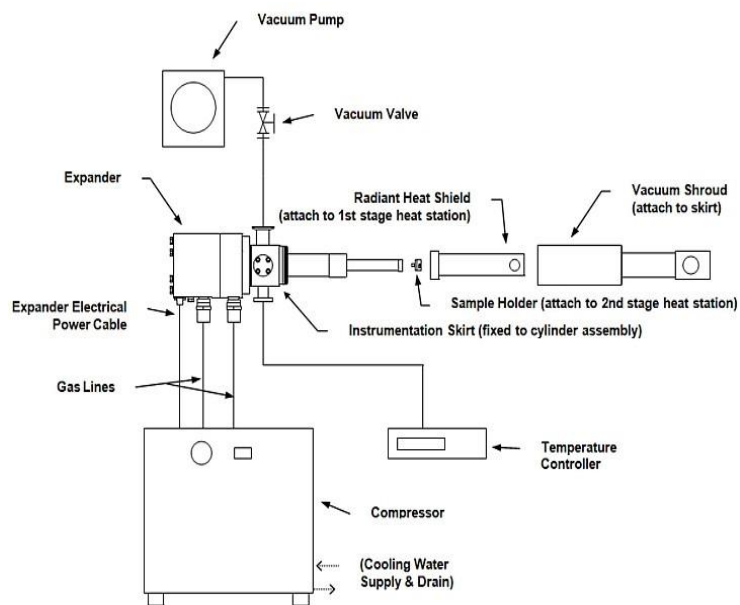


Figure 2.2: Schematic diagram for cryo-system assembly



Helium Compressor



Cryostat

Figure 2.3: Cryostat and its associated units

Sample Introduction Assembly

One of the requirements of the sample to be studied in the matrix is that it should have a reasonable vapor pressure at easily attainable temperatures. The mixing chamber is first filled with the matrix gas which is connected to the cryostat through a copper tubing. The flow of matrix gas is controlled during deposition using a needle valve (Model: EVN 116, Pfeiffer Vacuum). In all the experiments done in this work, the sample to be studied was cooled using a liquid nitrogen and ethanol cooling bath to an appropriate temperature to attain the desired vapor pressure so that the required matrix to sample ratio could be prepared. The experiments were done with a double jet setup, in which the sample holder is placed near the deposition window, and sample and matrix gas are introduced through two different nozzles.

FTIR Spectrometer

A Bruker Tensor 27 FTIR Spectrophotometer (Fig.2.5) was used to study the matrix isolated species. The spectra were recorded in the region 4000 to 400 cm^{-1} at a resolution of 0.5 cm^{-1} . In all the experiments eight scans were coadded to obtain a good signal-to-noise ratio. Fig. 2.6 shows a home built matrix isolation set up.



Figure 2.4: Diffusion Pump



Figure 2.5: FTIR Spectrometer

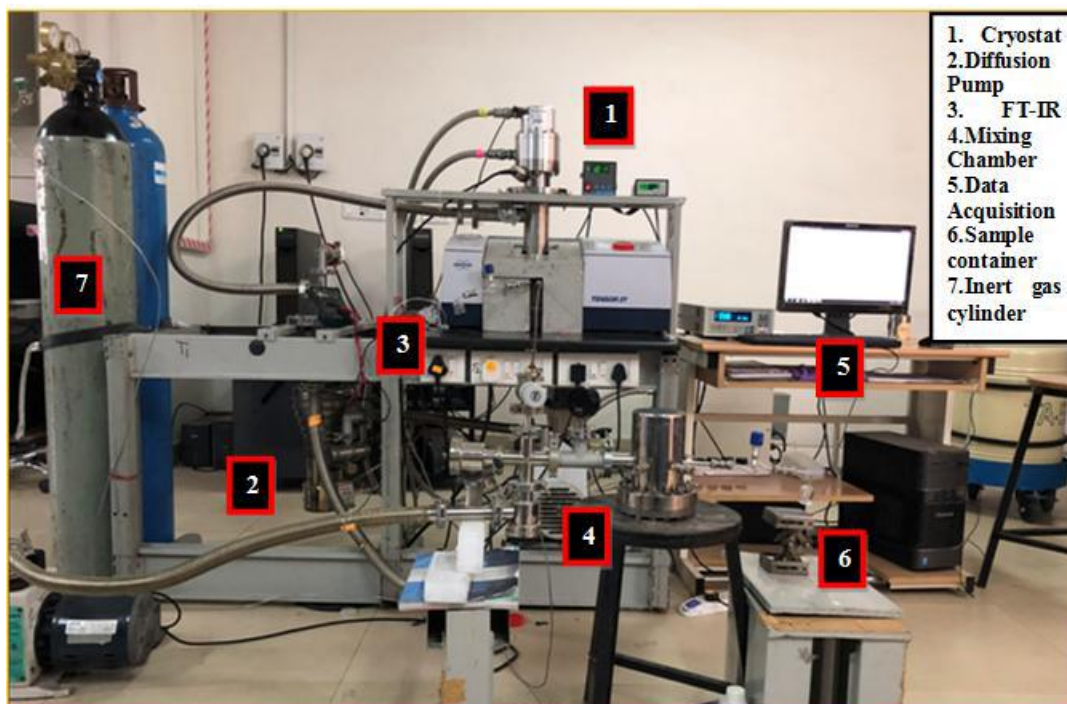


Figure 2.6: Home built Matrix Isolation setup

Chapter – 3

Computational Method

Introduction

Quantum chemical computational methods have become a useful tool for solving interesting chemical problems and reaction mechanism. One can simulate atomic or molecular models using computers to study their various chemical properties. The high computational speed of molecular mechanics allows for its use in procedures such as molecular dynamics, conformational energy searching, and docking that requires a large number of energy evaluation.

Computational techniques employed in this work use electronic structure calculation in which the nuclei within the molecule are treated as stationary particles surrounded by moving electrons. *Ab initio* (Latin; meaning – from the beginning) methods are solely based on theoretical principals with no approximation based on experimental data.

The Gaussian09²⁰ suite of programs, used for this work, is the most widely used program package for performing electronic structure calculations. Computations of optimized molecular geometry and vibrational spectra are typically carried out with the initial molecular geometry provided in the Z matrix format or Cartesian coordinate form. AIM2000²¹ software was also used for some calculations and analysis to study the nature of inter and intra molecular interactions. Natural Bond Orbital (NBO) analysis was also done to understand the orbital interactions within the molecule.

Levels of theory

A variety of theoretical methods are used to perform the electronic structure calculations, each with different sets of approximations. The choice of the theory is dependent on the system to be studied. Table 3.1 here provides an example of different methods that can be used in Gaussian09.

Using the *ab initio* method, a wide variety of properties such as molecular energy, vibrational frequencies, and thermodynamic properties, etc. can be computed. The simplest of the *ab initio* methods is the Hartree Fock method. In this method the potential in which an electron moves is calculated by treating the average distribution of all the other electrons as a single source of potential. Due to this assumption, we get an uncorrelated system, and

this lack of electron correlation is the major drawback of this system.

Table 3.1: Levels of theories

Family of Theory	Example
Hartree Fock	HF
Møller-Plesset Perturbation Theory	MP2 MP3 MP4
Density Function Theory	B3LYP APFD CAM – B3LYP
Couple Cluster Methods	CCSD
Compound Models	CBS-QB3 G3, G4

The Møller Plesset (MP) Perturbation method, which is majorly used in this work, improves the HF method by using the perturbation theory method to determine the electron correlation energy corrections. The perturbation can be truncated at second order (MP2), third order (MP3) or even higher orders (MP4 and MP5).

Density functional theory (DFT) provides an alternative approach to electron correlation. Here the electron correlation is accounted for by modifying the energy functionals. B3LYP (Beckee-Lee-Yang-Parr) is a common DFT method, also used for this work, which includes some HF exchange terms. DFT methods are computationally less expensive relative to the MP methods.

Basis set

Basis sets provide a collection of mathematical functions. These mathematical functions are used to build the quantum mechanical wavefunction for the molecular system. If seen physically, basis set define the region in space to which each electron is restricted. Larger basis sets have lesser constraints on this region of space for the electrons. A large number of basis sets are available to a computational chemist, and there is a trade-off between the size and the intricacy of the basis set with the computational time and resource needed. Some examples of the basis sets are given in Table 3.2.

Table 3.2: Basis Sets

Type	Example
Minimal Basis Set	STO-3G STO-6g
Split Valence Basis Set	4-21G 6-31G
Correlation Consistent Basis Set	cc-pVDZ cc-pVQZ cc-pVTZ
Polarization Consistent Basis SET	augpc-n

In the split-valence type basis sets, the valence orbitals are represented by two sets of functions. The system of notation used for it is A-BC, where A is the number of the Gaussians functions representing each core basis function and B and C are the Gaussian functions representing the split valence basis functions. Polarized basis sets add orbitals with angular momentum exceeding what is required. Diffused basis sets are used for the larger systems where the electrons are relatively far away from the nuclei. In contrast to the split-valence basis sets, double zeta (DZ) and triple zeta (TZ) basis sets split all the orbitals into either two and three sets of functions, respectively. These basis sets already contain polarization functions, and diffuse functions are added by using the prefix “aug-” for augmented. The general philosophy used in choosing a basis set is dictated by the nature of the problem. The biggest (and therefore the best) basis set available for the molecule of interest, consistent with the need to obtain meaningful results within an acceptable timescale is generally preferred for the calculations. For the calculations here in this work aug-cc-pVDZ basis set was used. It belongs to the family of ‘correlation- consistent polarized’ basis sets, and the ‘V’ indicates that they are valence only basis sets. ‘DZ’ indicates double zeta which means that it has two basis functions for each valence orbital.

Geometry Optimization and Frequency Calculation

Geometry optimization is the first step in studying a molecule computationally. Geometry optimization is the process of finding a minimum energy structure on the potential energy surface (stationary points) in the neighborhood of the initially assumed geometry. For a molecule with several conformations, one has to repeat the procedure of local minimum search for each possible conformation by starting with different initial trial

geometries and, thus locate the global minimum (Fig. 3.1).

It is possible that the computationally obtained stationary point (SP) could be a global minimum, a local minimum or a saddle point(maximum). To distinguish between a minimum and a saddle point, harmonic frequency calculations were performed on optimized structures as for a minimum; all the computed frequencies should be positive whereas structures with one or more imaginary frequencies correspond to a saddle point.

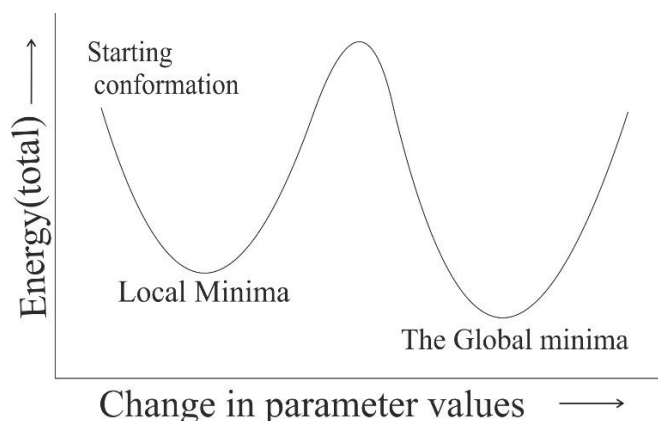


Figure 3.1: Geometry optimization to find minima

While studying the weak chemical interaction between two species; one needs to see whether that interaction leads to stability. Stabilization energy can be calculated as,

$$\Delta E = E_{\text{complex}} - E_{\text{monomer1}} - E_{\text{monomer2}}$$

E_{complex} = Energy of the stabilized geometry of the interacting complex

E_{monomer} = Energy of the optimized geometry of monomer

For a stable complex, the value of ΔE is negative.

The energy calculated above is referred to as uncorrected energy and must be corrected for zero-point correction. The zero-point energy is $0.5\sum hv$, where v is the frequency of a given normal mode of vibration and h is the Planck's constant. The energy hence obtained is referred to as zero-point corrected energy (E_{ZPCE}).

Natural Bonding Orbital Analysis

To understand the role of the delocalization interactions in the stability of the aminoethanol-water complexes as well as the intramolecular interactions in the aminoethanol, natural bond orbital (NBO) analysis was performed. The second order perturbation energies E_2 provided in the NBO analysis can be considered as the residual delocalization effect. These orbital energies are a function of both, the energy difference

between the two natural orbitals of the donor and the acceptor sites $E(j) - E(i)$ and their orbital overlap coefficients $F(i,j)$. The NBO analysis of aminoethanol and its complexes with water were carried out at MP2/aug-cc-pVDZ level of theory.

AIM Analysis

Atoms in Molecules (AIM) theory, developed by Bader and his co-workers²¹, is a method to observe the topology of electron density in space. The wavefunction file for the optimized geometry of the system, generated using the Gaussian09, is used as the input to the AIM2000 software which then develops the electron density plot for that geometry of the system. From this electron density plot, bond critical points, charge density $\rho(r)$, Laplacian of charge density $\nabla^2 \rho$, which is the sum of the three Hessian eigenvalues ($\lambda_1, \lambda_2, \lambda_3$) were estimated. The point in space where the derivative of the charge density vanishes is defined as a critical point (CP). A critical point between two atoms is a (3, -1) critical point; a (3, +1) is a ring critical point and (3, +3) corresponds to a cage. In general, a CP is described as (ω, σ) , where ω (rank), is the number of non-zero eigenvalues and σ (signature) is the algebraic sum of the signs of eigenvalues. The Laplacian of the charge density provides a useful characterization of the charge density distribution in the internuclear region. According to Koch and Popelier²², for closed-shell interactions, such as hydrogen bonded complexes, van der Waal complexes, and ionic systems, the charge density at the bond critical point is quite small and the Laplacian the charge density is positive. A negative sign of Laplacian is indicative of a shared shell type interaction suggesting that there is a concentration of electronic charge between the pair of atoms involved in bonding.

Chapter 4

Results and Discussions

Aminoethanol Conformations

Aminoethanol conformations have been a subject of investigation earlier, and computational and experimental work has been done before on it. This section here presents the results for the computational and matrix isolation infrared experiments done to understand the conformations of aminoethanol.

Computational Results

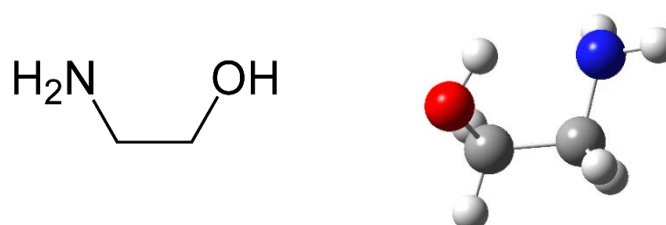


Figure 4.1: Chemical structure of aminoethanol

The aminoethanol molecule (Fig. 4.1) can exist in multiple possible conformations due to the presence of multiple freely rotatable single bonds. The structures were optimized at B3LYP and MP2 levels of theory using aug-cc-pVDZ basis set. The conformers obtained were classified into two major class viz. gauche and trans based on the orientation of the O-C-C-N dihedral angle in the optimized structures. The aminoethanol does not adopt eclipsed form because of steric reasons.

Thirteen conformers of aminoethanol were obtained by optimizing various initial geometries, as shown in fig. 4.3. The geometrical parameters for all 13 conformers have been provided in the appendix. The conformer nomenclature method used here is the same as followed by Radom et al.²³ (Fig. 4.2). The notation for all the conformers are based on three key dihedral angles: H-O-C-C, O-C-C-N and lpN-N-C-C (lpN denotes the lone pair on N) for example in g'gt, g' refers to opposite gauche($\sim -60^\circ$) angle for the H-O-C-C dihedral, g denotes O-C-C-N torsional angle is gauche($\sim 60^\circ$) and t denotes lpN-N-C-C dihedral is trans($\sim 180^\circ$). Out of these thirteen conformers, eight are gauche about the O-C-C-N dihedral angle, whereas the other five conformers are in trans form. The energies of all conformers, relative to the most stable form, computed at MP2 and B3LYP levels using the aug-cc-pVDZ basis set are listed in Table 4.1. All the 13 structures were obtained as a

minimum at both levels of theories with a similar relative energy ordering.

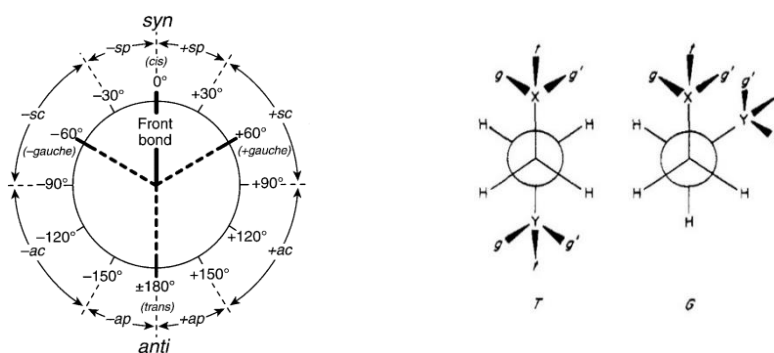


Figure 4.2: Nomenclature scheme for aminoethanol conformers

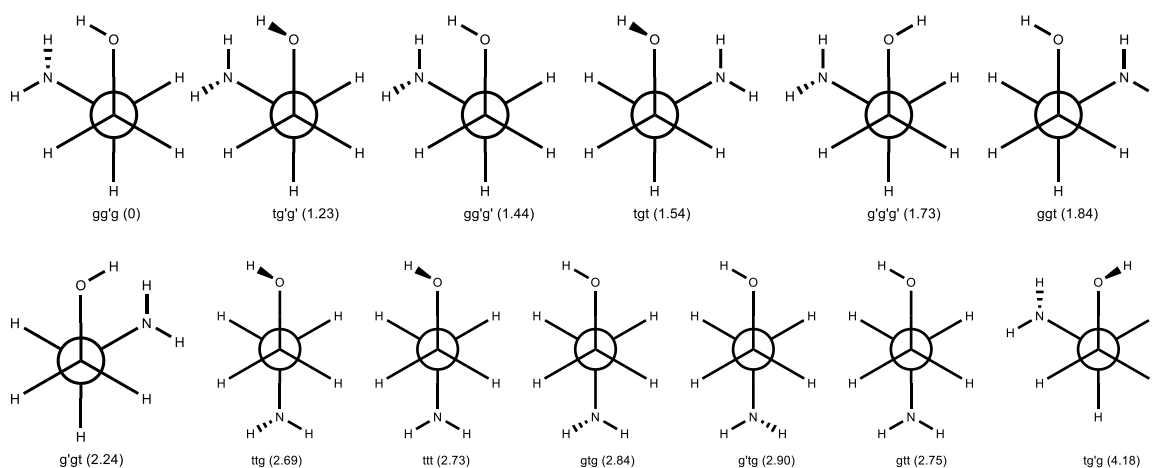


Figure 4.3: Conformations of Aminoethanol

It can be seen that the global minimum corresponds to a structure with $gg'g$ configuration and given that the next higher energy conformer is about 1.2kcal/mol above, the lowest energy structure contributes to more than 66% of the total population. In short, the global minimum dominated the chemistry of aminoethanol.

Reasons for conformational stability was next examined. Intramolecular hydrogen bonding interactions are often involved in conformational stability. Presence of such weak non-covalent interactions in the different conformers of aminoethanol was investigated by performing AIM analysis for the gauche backbone conformers. The AIM analysis for the conformers has been shown in Fig. 4.4 where the red dots on the bond path indicate the bond critical point for the respective covalent bond.

Table 4.1: Relative energy ordering for the conformers (kcal/mol)

Conformer	MP2/aug-cc-pVDZ	B3LYP/aug-cc-pVDZ
gg'g	0/0	0/0
tg'g'	1.50/1.23	1.50/1.22
gg'g'	1.63/1.44	1.74/1.38
tgt	1.92/1.54	1.59/1.40
g'g'g'	1.99/1.73	1.87/1.59
ggt	2.19/1.84	1.94/1.61
g'gt	2.72/2.24	2.37/1.95
ttg	3.10/2.69	2.72/2.34
ttt	3.20/2.73	2.75/2.28
gtt	3.22/2.75	2.79/2.33
gtg	3.26/2.84	2.87/2.48
g'tg	3.32/2.9	2.91/2.50
tg'g	4.83/4.18	4.4/3.77

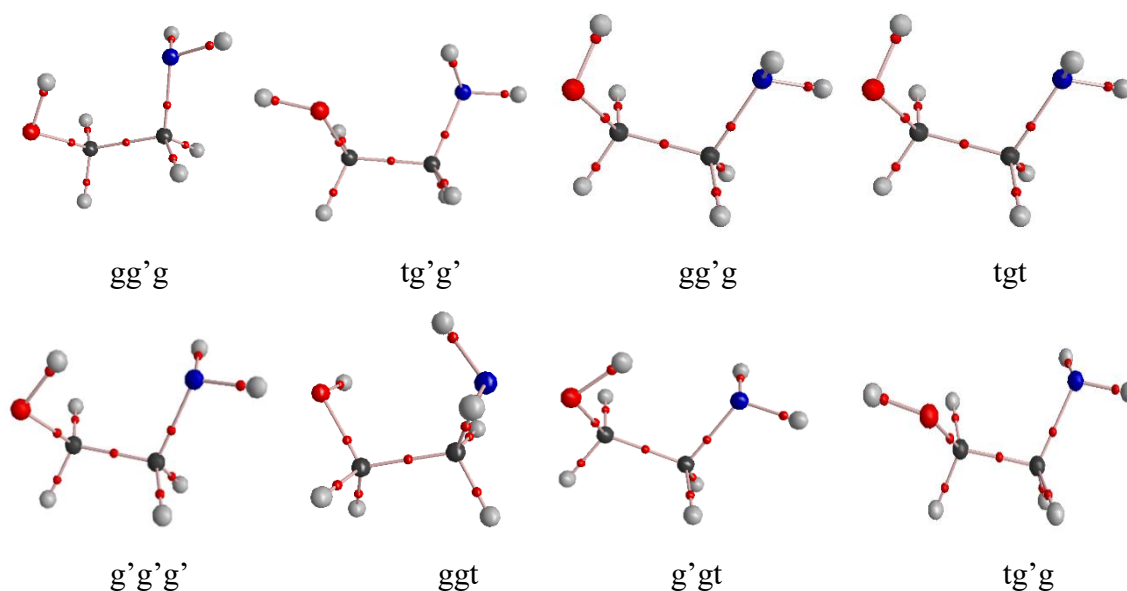


Figure 4.4: AIM analysis of Aminoethanol

As it can be seen in these figures, no bond critical point is observed along O-H \cdots N bond path, between the hydroxyl and the amino moieties. Thus, AIM analysis does not indicate the presence of the intramolecular hydrogen bond in different conformers of aminoethanol, and hence it can be assumed that intramolecular hydrogen bonding interactions do not play a role in the conformational stability.

The role of orbital delocalization interactions in the stability of aminoethanol conformers was then studied by performing natural bond orbital (NBO) analysis, on the four lowest energy structures. The stability due to the interaction of specific orbitals was rationalized based on the second order perturbation energy(E_2). Table 4.2 here shows the NBO analysis for the 4 lowest energy conformers, indicating the values for the second order perturbation energies (E_2), energy difference between the donor and the acceptor orbitals ($E(j) - E(i)$) and the overlap between the two orbitals $F(i,j)$. The second order perturbation energy values in Table 4.2 are only shown for those above the threshold of 0.5kcal/mol. As it can be seen that, for the lowest energy structure(gg'g), the contribution of the lone pair of Nitrogen (N7) to the anti-bonding orbital(σ^*) of the hydroxyl (O-H) group is 3.45kcal/mol. It is thus suggesting the presence of a weak intramolecular hydrogen bond between N(7) and H(11)-O(10) in the most stable conformer. It must be noted that AIM analysis did not reveal the presence of this interaction.

Presence of the intramolecular hydrogen bonding interaction in gg'g conformer, indicated by NBO and not by AIM, is manifested as a redshift in the computed vibrational frequency of O-H stretching mode of this conformer, compared with the O-H mode in the other conformers. A comparison between the O-H stretching frequency of the gg'g conformer and conformers with a relative higher energy shows a redshift of nearly 110 wavenumbers.

This observation supports the presence of intramolecular hydrogen bonding in the lowest energy conformer of aminoethanol, i.e., gg'g.

These results are pretty much in agreement with the previous studies done on aminoethanol conformations. Computations done by Thomsen et al.¹⁵ on aminoethanol shows similar results in terms of conformer structures found, and the global minima is the same as the one observed through our work. They did not observe any hydrogen bonding in any of the aminoethanol conformers by AIM analysis although they did Non-Covalent Interaction(NCI) analysis which does show hydrogen bonding in the lowest energy structure just like we observed here in our analysis.

Table 4.2: NBO analysis for aminoethanol

Conformer	Donor	Acceptor	E_2 (kcal/mol)	$E(j) - E(i)$ (au)	$F(I,j)$ (au)
gg'g	lp N(7)	σ^* C(1)-H(2)	0.65	1.18	0.025
	lp N(7)	σ^* C(1)-C(4)	2.59	1.15	0.049
	lp N(7)	σ^* C(4)-H(6)	9.32	1.16	0.093
	lp N(7)	σ^* O(10)-H(11)	3.45	1.23	0.059
	lp1 O(10)	σ^* C(1)-H(2)	1.92	1.51	0.048
	lp1 O(10)	σ^* C(1)-C(4)	2.6	1.48	0.056
	lp2 O(10)	σ^* C(1)-H(2)	1.25	1.15	0.024
	lp2 O(10)	σ^* C(1)-H(3)	11.04	1.12	0.1
	lp2 O(10)	σ^* C(1)-C(4)	3.77	1.12	0.058
	lp2 O(10)	σ^* C(4)-H(6)	0.77	1.12	0.026
tg'g'	lp N(7)	σ^* C(1)-C(4)	1.00	1.14	0.03
	lp N(7)	σ^* C(4)-H(5)	1.85	1.16	0.041
	lp N(7)	σ^* C(4)-H(6)	10.63	1.15	0.099
	lp1 O(10)	σ^* C(1)-H(3)	2.09	1.52	0.051
	lp1 O(10)	σ^* C(1)-C(4)	1.25	1.52	0.039
	lp1 O(10)	σ^* C(4)-H(5)	0.60	1.53	0.027
	lp2 O(10)	σ^* C(1)-H(2)	9.22	1.16	0.092
	lp2 O(10)	σ^* C(1)-H(3)	5.66	1.16	0.072
gg'g'	lp N(7)	σ^* C(1)-H(2)	0.76	1.17	0.027
	lp N(7)	σ^* C(1)-C(4)	2.95	1.15	0.052
	lp N(7)	σ^* C(4)-H(5)	8.58	1.16	0.089
	lp1 O(10)	σ^* C(1)-H(2)	2.06	1.53	0.05
	lp1 O(10)	σ^* C(1)-H(3)	2.39	1.51	0.054
	lp1 O(10)	σ^* C(1)-C(4)	0.57	1.5	0.026
	lp2 O(10)	σ^* C(1)-H(3)	5.19	1.15	0.069
	lp2 O(10)	σ^* C(1)-C(4)	8.23	1.14	0.087
	lp2 O(10)	σ^* C(4)-H(6)	1.32	1.15	0.035

tgt	lp N(7)	σ^* C(1)-H(2)	1.25	1.12	0.024
	lp N(7)	σ^* C(1)-C(4)	9.83	1.13	0.094
	lp N(7)	σ^* C(4)-H(5)	1.1	1.15	0.032
	lp N(7)	σ^* C(4)-H(6)	1.89	1.15	0.042
	lp1 O(10)	σ^* C(1)-H(2)	0.99	1.52	0.035
	lp1 O(10)	σ^* C(1)-H(3)	1.61	1.51	0.044
	lp1 O(10)	σ^* C(1)-C(4)	1.34	1.52	0.04
	lp1 O(10)	σ^* C(4)-H(5)	0.62	1.52	0.028
	lp2 O(10)	σ^* C(1)-H(2)	8.38	1.15	0.088
	lp2 O(10)	σ^* C(1)-H(3)	7.27	1.15	0.082

Experimental Results

The results of the matrix isolation IR experiments of aminoethanol are provided in this section. The vapor pressure of aminoethanol is about 0.4mm Hg at 20°C²⁴. The sample bulb containing aminoethanol was placed close to the cryostat to achieve a significant amount of sample deposited on the KBr window. The experiments were done in both nitrogen and argon as matrix gas.

The matrix isolated IR spectra of aminoethanol in Nitrogen matrix is shown in Fig. 4.5. The experimental results were corroborated with the computed spectra of lowest energy conformer. Synthetic spectra were generated using SYNSPEC package. The computed spectra were generated using the computed vibrational wavenumbers and the intensities of the various modes, computed at MP2/aug-cc-pVDZ level of theory. The experiments were done at different temperatures in the range -20°C to -35°C, to achieve different vapor pressures of aminoethanol, hence resulting in different concentrations of the sample being deposited.

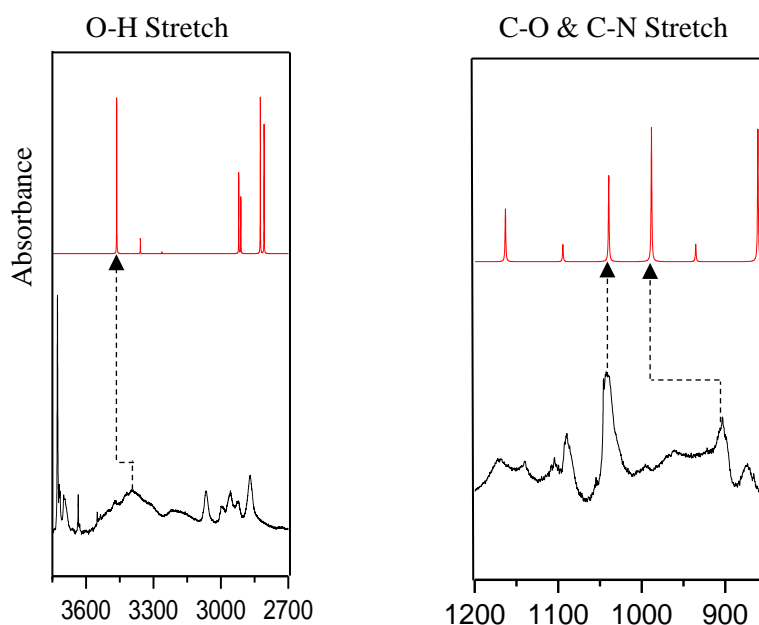
The exact concentration of aminoethanol could not be known to get the exact matrix to sample ratio in this case as the setup was such that the matrix gas was deposited through the mixing chamber gas line while the sample bulb was attached to near the window (double jet setup). The variation in the concentrations helped in confirming the vibrational assignments. The computed wavenumbers were scaled using a scaling factor of 0.9302. The feature corresponding to the O-H stretch is observed at 3471.6 cm⁻¹, is found to be in good agreement with the computed wavenumber of the lowest energy conformer, found to be 3469.9cm⁻¹. The features observed at 1041.4 cm⁻¹ and 903.7 cm⁻¹ corresponds to the symmetric and asymmetric stretches of C-O and C-N bonds. These experimental features

are found to be in good agreement with the computed wavenumber. The vibrational assignments between computations and the experiments presented in Table 4.3. Thus, the assignment between experimental and computed wavenumbers suggests the presence of only the lowest energy conformer in our experiment. Upon annealing the matrix to 25K from 12K for 30 minutes, no significant change in the spectral features was observed.

Table 4.3: Vibrational feature assignment Aminoethanol in Nitrogen matrix as per scaled computed frequencies obtained at MP2/aug-cc-pVDZ level of theory

Experimental Frequency	Computed Frequency	Intensity (computed)	Vibrational Mode Assignment
3471.4	3464.9	64.5	O-H stretch
1041.4	1039.9	33.9	Symmetric C-O & C-N stretch
903.7	988.8	52.8	asymmetric C-O & C-N stretch

Figure 4.5: Matrix isolation IR spectrum of aminoethanol (black) in nitrogen matrix along with the computed scaled spectra (red) for gg'g showing the (a) O-H stretching frequency region; (b) C-O & C-N stretching frequency region.



The IR spectrum of the matrix isolated aminoethanol, in the argon matrix, is shown in Fig. 4.6. The vibrational assignment between the computed and the experimental

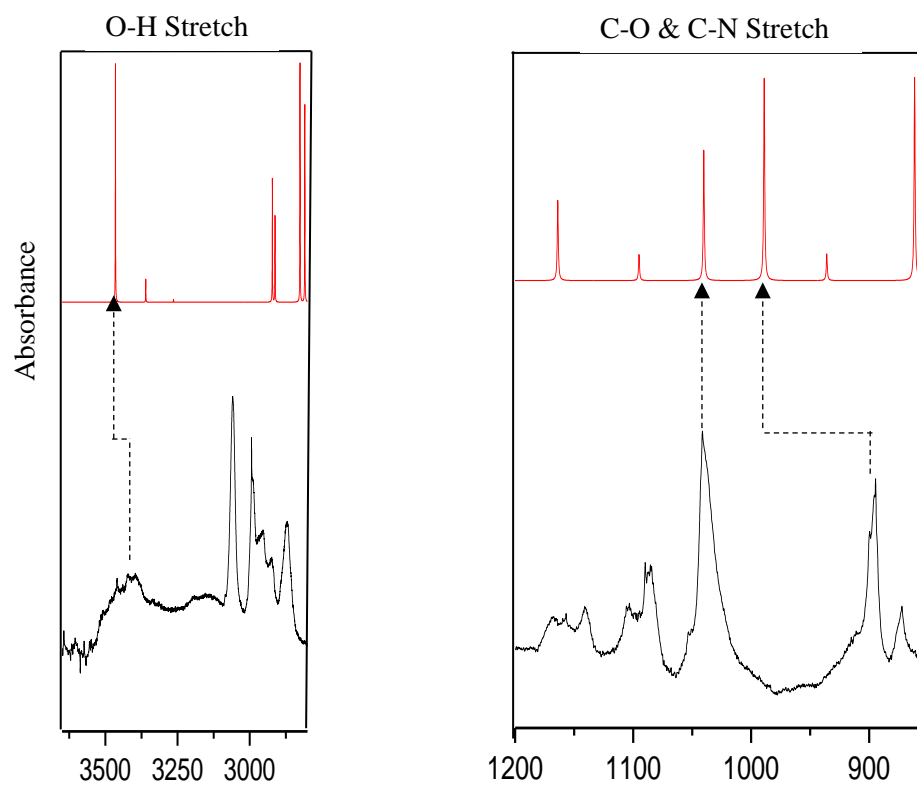
wavenumber suggest the presence of only the lowest energy conformer in our experiment. The feature corresponding to the O-H stretch is observed at 3462cm^{-1} . The features observed at 1040cm^{-1} and 897cm^{-1} corresponds to the symmetric and asymmetric stretches of C-O and C-N bonds. The corroborated results for the experimental and the computed frequencies along with their assignments are listed in Table 4.4.

A common feature of the O-H feature in both the matrices is the broadness of this feature. The broadness of the O-H stretching feature can be attributed to the presence of intramolecular hydrogen bond in aminoethanol. Other possible reasons for peak broadening could be complex formation with water, but such a possibility was ruled out, as the intensity of the observed feature does not increase on annealing. The peak broadening due to site effects of the matrix is also unlikely, as it is observed in both nitrogen as well as the argon matrix.

Table 4.4: Vibrational feature assignment aminoethanol in the argon matrix as per scaled computed frequencies obtained at MP2/aug-cc-pVDZ level of theory

Experimental Frequency	Computed Frequency	Intensity (computed)	Vibrational Mode Assignment
3462.2	3465.1	64.5	O-H stretch
1040.8	1040.0	33.9	Symmetric C-O C-N stretch
897.6	988.8	52.8	Asymmetric C-O C-N stretch

Figure 4.6: Matrix isolation IR spectrum (black) of aminoethanol in Argon matrix along with the computed scaled spectra (red) for gg'g showing the (a) O-H stretching frequency region; (b) C-O & C-N stretching frequency region.



Aminoethanol-Water Complex

Aminoethanol molecule has several possible sites for interacting with the water molecule as it has a hydroxyl and an amino group. The presence of O-H and NH₂ groups provide both proton donating and proton accepting sites, to a large number of possibilities for the aminoethanol-H₂O complex. It was therefore considered interesting to study these complexes.

The geometries for various complexes with water were computed at MP2/aug-cc-pVDZ level of theory, using the lowest energy conformer for aminoethanol (gg'g). The lowest energy structure is the one where O-H group of aminoethanol is the proton donor and water is proton acceptor along with another interaction in the same structure where N is proton acceptor, and water is proton donor. The optimized structures for the complexes are presented in Fig. 4.7. The stabilization energies for the complexes are given in Table 4.5. AIM analysis of these structures was also performed, and the results are shown in Fig. 4.7. Table 4.6 shows the electron density parameter at critical points obtained in the AIM analysis.

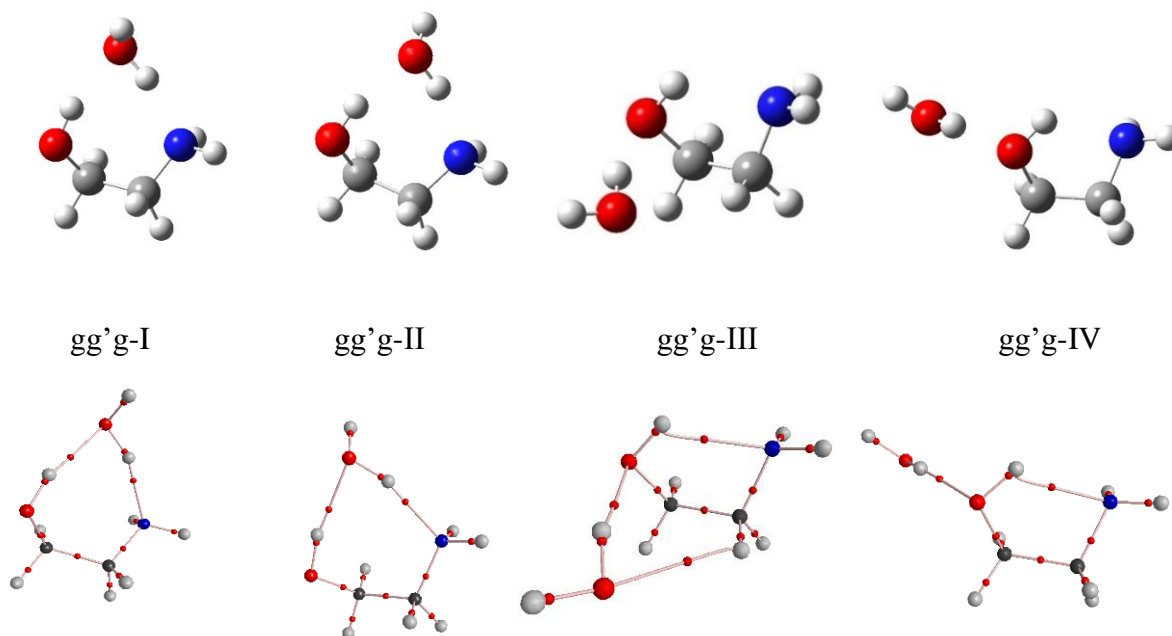


Figure 4.7: Complexes of aminoethanol with water(above). AIM analysis for aminoethanol- water complexes (bottom)

The first complex, gg'g-I, shows two intermolecular hydrogen bonding interactions, one between N of aminoethanol (proton acceptor) and water (proton donor); second interaction is between O of aminoethanol (proton donor) and water (proton acceptor). This complex of aminoethanol and water was found to be the most stable.

The complex gg'g-II is similar to the complex gg'g-I, with a small variation in the orientation of the water molecule with respect to the aminoethanol molecule, thus resulting in the difference in energy of the two complexes. Complex gg'g-III shows three interactions, as indicated by AIM analysis, i.e., intramolecular N···· O-H hydrogen bond, intermolecular hydrogen bond involving water (proton donor) and oxygen of aminoethanol (proton acceptor) and a secondary interaction between the oxygen of water and hydrogen attached to the sp³-carbon. The fourth complex shown here shows two interactions, one intramolecular hydrogen bonding similar to the previous gg'g-III structure and other intermolecular hydrogen bonding where water is the proton donor and oxygen of aminoethanol is the proton acceptor.

All these inter, as well as intra molecular interactions found, were confirmed using NBO analysis as well. Table 4.7 shows the orbital interaction parameter obtained in NBO analysis, for these complexes.

Table 4.5: Interaction energy (zero point corrected in kcal/mol) for aminoethanol water complex computed at MP2/aug-cc-pVDZ level of theory.

Complex Structure	Interaction energy
gg'g-I	6.92
gg'g-II	6.50
gg'g-III	5.94
gg'g-IV	5.16


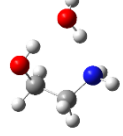
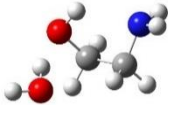
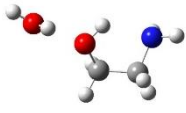
Table 4.6: AIM analysis, showing the electron density and Laplacian values, for the aminoethanol water complexes.

Complex Structure	Interaction	$\rho(r_c)$	Laplacian
gg'g-I	N···· H-O	0.0369	-0.0265
	O···· H-O	0.0285	-0.0242
gg'g-II	N···· H-O	0.0373	-0.0266
	O···· H-O	0.0288	-0.0253
gg'g-III	N···· H-O	0.0226	-0.0185
	O····H-O	0.0306	-0.0267
	N····H-C	0.0071	-0.0073
gg'g-IV	N····H-O	0.0229	-0.0188
	O····H-O	0.0297	-0.0263

Previously some computational work has been done on the aminoethanol- water system. A computational study done by Tubergen et al.¹⁶ on this system at MP2/6-311++G(d,p) level shows a similar set of structures corresponding to the complex. The global minima and the second lowest energy structure are the same as found in our work, as the rotational constants for the structures are in fair agreement up to one decimal point.

Another computational study has been done by Haufa et al.¹⁷ at B3LYP/6-311G(d,p) shows the complex structure with single intermolecular interaction where water is donation proton to the O of aminoethanol to be the global minimum. This structure corresponds to the fourth structure in energy ordering (gg'g-IV) in our study. Our work based on AIM and NBO analysis provides a more detailed analysis of the structure of the complexes.

Table 4.7: NBO analysis for aminoethanol-water complex

Complex Structure	Donor	Acceptor	E ₂ (kcal/mol)	E(j) -E(i) (au)	F(i,j) (au)
gg'g-I 	lpN(7)	σ^* O(12)H(14)	23.2	1.23	0.152
	lpO(12)	σ^* O(10)H(11)	14.18	1.34	1.89
gg'g-II 	lpN(7)	σ^* O(12)H(14)	23.87	1.23	0.154
	lpO(12)	σ^* O(10)H(11)	14.49	1.37	0.126
gg'g-III 	lpN(7)	σ^* O(10)H(11)	5.42	1.21	0.073
	lpO(10)	σ^* O(12)H(14)	11.92	1.31	0.112
	lp1O(12)	σ^* C(1)H(3)	0.14	1.51	0.013
gg'g-IV 	lpN(7)	σ^* O(10)H(11)	5.46	1.21	0.073
	lpO(12)	σ^* O(10)H(11)	11.07	1.3	0.108

Chapter – 5

Conclusions

To study the conformations of aminoethanol the technique of matrix isolation infrared spectroscopy along with *ab initio* calculations was used. The aminoethanol- water complex system was studied computationally. For all the conformers the geometry optimization was done at MP2 and B3LYP levels of theories using aug-cc-pVDZ as basis set. All further computations were carried out at MP2/aug-cc-pVDZ level.

In the conformational analysis, thirteen structures were found to be minima out of which the lowest energy structure(gg'g) was observed experimentally. AIM analysis although shows an absence of intramolecular hydrogen bonding in these conformers but the NBO analysis shows some interaction in the gg'g structure. This interaction is further manifested as a significant redshift in the computed OH stretching frequency observed for gg'g compared to other conformers. These results are in agreement with the work done previously on the aminoethanol molecule. The computational results of previous studies show the same structure to be the global minima as found through our calculations. Also, this work is also in agreement with the earlier work regarding the presence of a hydrogen bond in the lowest energy structure.

Experimentally, in previous works, the lowest energy structure has been observed in the gas phase and matrix isolation spectroscopy.

The lowest energy conformer observed experimentally(gg'g) was further used for the aminoethanol water complex study computationally. Structures involving multiple intermolecular hydrogen bonding were found to be more stable than the other structures, which involved only one interaction. The lowest energy structure of the complex system is the one where the O of

aminoethanol is the proton donor and water is the proton acceptor along with another interaction in which N is the proton acceptor, and the water is the proton donor. This observed structure is similar to the structure reported earlier through computational studies.

Future Scope

The aminoethanol water system has been studied here computationally which can be followed up by experimental work. Matrix isolation IR experiments can be done for aminoethanol with water and also D₂O at different concentrations.

Work on the methanol – aminoethanol systems will also be interesting to do as the methyl group is likely to introduce C-H hydrogen bonded interactions.

References:

- (1) Arunan, E.; Desiraju, G. R.; Klein, R. A.; Sadlej, J.; Scheiner, S.; Alkorta, I.; Clary, D. C.; Crabtree, R. H.; Dannenberg, J. J.; Hobza, P.; et al. Definition of the Hydrogen Bond (IUPAC Recommendations 2011). *Pure Appl. Chem.* **2011**, 83 (8), 1637–1641. <https://doi.org/10.1351/pac-rec-10-01-02>.
- (2) Donaldson, D. J.; Tuck, A. F.; Vaida, V. Atmospheric Photochemistry via Vibrational Overtone Absorption. *Chem. Rev.* **2003**. <https://doi.org/10.1021/cr0206519>.
- (3) Vaida, V.; Feierabend, K. J.; Rontu, N.; Takahashi, K. Sunlight-Initiated Photochemistry: Excited Vibrational States of Atmospheric Chromophores. *Int. J. Photoenergy* **2008**. <https://doi.org/10.1155/2008/138091>.
- (4) Vaida, V. Spectroscopy of Photoreactive Systems: Implications for Atmospheric Chemistry. *J. Phys. Chem. A* **2009**. <https://doi.org/10.1021/jp806365r>.
- (5) Aloisio, S.; Francisco, J. S. Radical-Water Complexes in Earth's Atmosphere. *Acc. Chem. Res.* **2000**. <https://doi.org/10.1021/ar000097u>.
- (6) Nielsen, C. J.; D'Anna, B.; Dye, C.; Graus, M.; Karl, M.; King, S.; Maguto, M. M.; Müller, M.; Schmidbauer, N.; Stenström, Y.; et al. Atmospheric Chemistry of 2-Aminoethanol (MEA). *Energy Procedia* **2011**, 4 (1), 2245–2252. <https://doi.org/10.1016/j.egypro.2011.02.113>.
- (7) Krueger, P. J.; Mettee, H. D. SPECTROSCOPIC STUDIES OF ALCOHOLS: VI. INTRAMOLECULAR HYDROGEN BONDS IN ETHANOLAMINE AND ITS O - AND N -METHYL DERIVATIVES. *Can. J. Chem.* **2006**. <https://doi.org/10.1139/v65-411>.
- (8) Mulla, S. T.; Jose, C. I. Intramolecular Hydrogen Bonding and Intermolecular Association of Amino Alcohols. *J. Chem. Soc. Faraday Trans. 1 Phys. Chem. Condens. Phases* **1986**. <https://doi.org/10.1039/F19868200691>.
- (9) Räsänen, M.; Aspiala, A.; Homanen, L.; Murto, J. IR-Induced Photorotamerization of 2-Aminoethanol in Low-Temperature Matrices. AB Initio Optimized Geometries of Conformers. *J. Mol. Struct.* **1982**. [https://doi.org/10.1016/0022-2860\(82\)90060-6](https://doi.org/10.1016/0022-2860(82)90060-6).
- (10) Przeslawska, M.; Melikowa, S. M.; Lipkowski, P.; Koll, A. Gas Phase FT-IR Spectra and Structure of Aminoalcohols with Intramolecular Hydrogen Bonds: I.

- The Shape of the $\nu(\text{OH})$ Vibrational Bands in $\text{R}_2\text{NC}_3\text{H}_6\text{OH}$ ($\text{R} = \text{H}, \text{CH}_3$). *Vib. Spectrosc.* **1999**. [https://doi.org/10.1016/S0924-2031\(99\)00023-5](https://doi.org/10.1016/S0924-2031(99)00023-5).
- (11) Omura, Y.; Shimanouchi, T. Skeletal Deformation Vibrations and Rotational Isomerism of Ethylenediamine and Monoethanolamine. *J. Mol. Spectrosc.* **1975**. [https://doi.org/10.1016/0022-2852\(75\)90307-0](https://doi.org/10.1016/0022-2852(75)90307-0).
- (12) Penn, R. E.; Curl, R. F. Microwave Spectrum of 2-Aminoethanol: Structural Effects of the Hydrogen Bond. *J. Chem. Phys.* **1971**. <https://doi.org/10.1063/1.1676133>.
- (13) Leavell, S.; Steichen, J.; Franklin, J. L. Photoelectron Spectra of Intramolecularly Hydrogen Bonded Compounds. *J. Chem. Phys.* **1973**. <https://doi.org/10.1063/1.1680631>.
- (14) Liu, Y.; Rice, C. A.; Suhm, M. A. Torsional Isomers in Methylated Aminoethanols - A Jet-FT-IR Study. *Can. J. Chem.* **2004**. <https://doi.org/10.1139/v04-046>.
- (15) Thomsen, D. L.; Axson, J. L.; Schröder, S. D.; Lane, J. R.; Vaida, V.; Kjaergaard, H. G. Intramolecular Interactions in 2 - Aminoethanol and 3 - Aminopropanol. **2013**. <https://doi.org/10.1021/jp405512y>.
- (16) Tubergen, M. J.; Torok, C. R.; Lavrich, R. J. Effect of Solvent on Molecular Conformation: Microwave Spectra and Structures of 2-Aminoethanol van Der Waals Complexes. *J. Chem. Phys.* **2003**, *119* (16), 8397–8403. <https://doi.org/10.1063/1.1612919>.
- (17) Haufa, K. Z.; Czarnecki, M. A. Molecular Structure and Hydrogen Bonding of 2-Aminoethanol, 1-Amino-2-Propanol, 3-Amino-1-Propanol, and Binary Mixtures with Water Studied by Fourier Transform near-Infrared Spectroscopy and Density Functional Theory Calculations. *Appl. Spectrosc.* **2010**. <https://doi.org/10.1366/000370210790918445>.
- (18) Whittle, E.; Dows, D. A.; Pimentel, G. C. Matrix Isolation Method for the Experimental Study of Unstable Species. *The Journal of Chemical Physics.* 1954. <https://doi.org/10.1063/1.1739957>.
- (19) Jones, H. Advances in Cryogenic Engineering Volume 32. *Cryogenics (Guildf)*. **1987**. [https://doi.org/10.1016/0011-2275\(87\)90041-5](https://doi.org/10.1016/0011-2275(87)90041-5).
- (20) Frisch, M. J.; Trucks, G. W.; Schlegel, H. B.; Scuseria, G. E.; Robb, M. A.; Cheeseman, J. R.; Scalmani, G.; Barone, V.; Men-nucci, B.; Petersson, G. A.; Nakatsuji, H.; Caricato, M.; Li, X.; Hratchian, H. P.; Izmaylov, A. F.; Bloino, J.; Zheng, G.; Son-ne, D. J. *Gaussian 09, Revision A. 1; Gaussian; 2009*.

- (21) Bader, R. F. W. *Atoms in Molecules: A Quantum Theory*, International Series of Monographs on Chemistry. *Oxford Univ. Press. Oxford Henkelman G, Arnaldsson A, Jónsson H A fast robust algorithm Bader Decompos. Charg. density. Comput Mater Sci* **1994**.
- (22) Koch, U.; Popelier, P. L. A. Characterization of C-H-O Hydrogen Bonds on the Basis of the Charge Density. *J. Phys. Chem.* **1995**, *99* (24), 9747–9754.
<https://doi.org/10.1021/j100024a016>.
- (23) Radom, L.; Lathan, W. A.; Hehre, W. J.; Pople, J. A. Molecular Orbital Theory of the Electronic Structure of Organic Compounds. XVII. Internal Rotation in 1,2-Disubstituted Ethanes. *J. Am. Chem. Soc.* **1973**, *95* (3), 693–698.
<https://doi.org/10.1021/ja00784a008>.
- (24) Matthews, J. B.; Sumner, J. F.; Moelwyn-Hughes, E. A. The Vapour Pressures of Certain Liquids. *Trans. Faraday Soc.* **1950**. <https://doi.org/10.1039/tf9504600797>.

Appendix

The geometrical parameters for the thirteen optimized structures of aminoethanol obtained at MP2/aug-cc-pVDZ level are provided below in Table A.1, Table A.2 and Table A.3

Table A.1 : Dihedral angles for aminoethanol conformations

Conformer	Dihedral Angles				
	H11-O10-C1-C4	O10-C1-C4-N7	H8-N7-C4-C1	H9-N7-C4-C1	lpN7-N7-C4-C1
gg'g	41.49	-56.85	164.17	-77.99	43.089
tg'g'	170.41	-65.11	60.86	177.08	-61.03
gg'g'	72.73	-56.46	84.39	-159.81	-37.71
tgt	-177.13	60.93	-53.25	62.04	-175.61
g'g'g'	-71.46	-62.54	56.23	173.29	-
ggt	70.58	58.36	-49.08	65.71	-171.69
g'gt	-70.60	61.79	-64.96	54.33	174.68
ttg	176.69	177.69	169.15	-74.45	47.35
ttt	-179.97	-179.99	-58.73	58.74	180.00
gtt	64.18	178.04	-60.00	57.16	178.58
gtg	68.53	177.38	171.50	-72.04	49.73
g'tg	-65.05	-179.16	170.59	-72.38	49.03
tg'g	172.96	-71.49	169.65	-73.65	47.99

Table A.2 : Bond length in aminoethanol conformers

Conformer	C-O(Å)	C-N(Å)	N-H(Å)	O-H(Å)	C-C(Å)	O-N(Å)
gg'g	1.42	1.47	1.01	0.97	1.53	2.81
tg'g'	1.44	1.47	1.02	0.97	1.52	2.84
gg'g'	1.44	1.47	1.02	0.97	1.52	2.84
tgt	1.44	1.47	1.02	0.97	1.53	2.91
g'g'g'	1.44	1.47	1.02	0.97	1.52	2.9
ggt	1.44	1.47	1.02	0.97	1.53	2.98
g'gt	1.44	1.47	1.02	0.97	1.53	3.04
ttg	1.44	1.47	1.02	0.97	1.52	3.67
ttt	1.44	1.47	1.02	0.97	1.53	3.73
gtt	1.44	1.47	1.02	0.97	1.53	3.79
gtg	1.44	1.47	1.02	0.97	1.53	3.73
g'tg	1.43	1.47	1.02	0.97	1.53	3.73
tg'g	1.43	1.47	1.02	0.97	1.52	2.96

Table A.3 : Bond angles for aminoethanol conformations

Conformer	H-O-C	H-O-N
gg'g	104.41	110.29
tg'g'	108.35	110.29
gg'g'	103.21	110.43
tgt	108.47	109.77
g'g'g'	107.56	110.81
ggt	107.61	109.52
g'gt	107.53	111.08
ttg	108.15	110.06
ttt	108.39	110.46
ggt	107.76	110.42
gtg	107.71	109.92
g'tg	107.88	110.31
tg'g	108.19	109.99